Acta Cryst. (1984). B40, 555-560

An Electron Diffraction Study of a Pre-martensitic In–24 at.% Tl Alloy

BY T. R. FINLAYSON

Department of Physics, Monash University, Melbourne, Australia

P. GOODMAN

Division of Chemical Physics, CSIRO, Melbourne, Australia

A. OLSEN

Department of Physics, University of Oslo, Norway

P. NORMAN

Chisholm Insitute of Technology, Frankston, Australia

AND S. W. WILKINS

Division of Chemical Physics, CSIRO, Melbourne, Australia

(*Received* 28 *September* 1983; *accepted* 1 *May* 1984)

Abstract

An electron diffraction study has been made of the In-24 at.% Tl alloy at two temperatures, *viz* room temperature and approximately 193 K, the latter temperature being close to but just above the martensitic transition temperature, T_m. From a series of diffraction patterns, obtained by rotations about the [220]* vector from the principal [001] zone, a model for the diffuse scattering, which is surprisingly intense and of the same order of magnitude as that of the fundamental reflexions, can be reconstructed. From this model it could be concluded that the corresponding disorder in real space occurs within {111} planes, consistent with the expected pre-martensitic behavior. The strength of the diffuse scattering and hence the degree of disorder responsible adequately explains previously observed anomalies in pre-martensitic neutron diffraction intensities. The interpretation given here for the electron diffraction data differs in some important respects from that reported in an earlier study by Koyama & Nittono [*J. Jpn Inst. Met.* (1981), **45**, 869-877].

I. Introduction

In-Tl alloys in the composition range 15·5-31 at.% Tl form disordered alloys which are subject to a martensitic phase transformation from face centered cubic (f.c.c.) to face centered tetragonal (f.c.t.). The temperature of the transition, T_m, has a particularly steep dependence on alloy composition. T_m falls from 425 K for 15·5 at.% to near absolute zero for 31 at.% Tl (Nakanishi, 1979). The part played by transverse acoustic modes in the phase transition was first demonstrated by Gunton & Saunders (1973), who showed that such In-Tl alloys exhibit a marked softening of the $[\zeta\zeta 0]$ phonon branch with reduction in temperature to T_m simultaneously with a decrease in the shear modulus $\frac{1}{2}(c_{11} - c_{12})$.

More recently, a detailed neutron diffraction study of the martensitic transition in an In-25 at.% Tl alloy was made by Wilkins, Lehmann, Finlayson & Smith (1982). They found an anomalous decrease in diffracted intensity of low-order reflexions as T_m was approached from above. Specifically, in measuring the integrated intensity of the 200 diffraction peak as a function of temperature, these authors observed a very marked hysteresis in cycling through the critical temperature T_m. There was a particularly steep fall in scattered intensity in *decreasing* the temperature from room temperature towards T_m. A typical set of results is presented in Fig. 1. Wilkins *et al.* took such results and the observed decrease in the scale factor of the measured intensities to imply some kind of temperature-dependent 'inhomogeneity' in the single crystal at a submacroscopic level.

The present electron diffraction study was made in order to investigate the pre-martensitic behavior on the scale of microdiffraction. It was thought that the present composition studied, *viz* of 24 at.% Tl, was sufficiently close to that of 25 at.% used by Wilkins *et al.* that useful comparisons of behavior could be made.

An earlier combined X-ray and electron diffraction study of In-(18-30) at.% Tl was made by Nittono & Koyama (1981). Their experiments were carried out at room temperature and above. Using alloys

0108-7681/84/060555-06$01.50

transforming at elevated temperatures, they approached the martensitic transformation by heating and found an anomalous enhancement of thermal diffuse scattering near T_m. They also found X-ray topographic evidence for a metastable two-phase region over a 50 K range, when the alloys were heated through the critical temperature starting from room temperature (*i.e.* in the tetragonal phase). Limited studies were made by electron diffraction at room temperature and these showed a highly structured diffuse background, which they interpreted along the lines laid down by Honjo, Kodera & Kitamura (1964) for aluminium. However, although the streak patterns obtained from aluminium under conditions of extreme overexposure (or the Bragg peaks) bear some resemblance to the present ones, those from In-Tl are much stronger in intensity relative to the Bragg peaks, and are more sharply structured, so that their conclusions are not entirely satisfactory.

II. Sample preparation

An alloy of nominal composition In-24 at.% Tl was prepared from high-purity samples of the metals. The heavy oxide coating which forms on the surface of thallium was removed using a series of sulfuric acid solutions of increasing dilution. The components were alloyed together in an evacuated and sealed quartz tube by heating and shaking vigorously over a bunsen flame. The ingot was then rolled to form a strip of approximately 0·3 mm thickness which was heat treated in a dynamic vacuum for 24 h at 393 K. Further thinning of the sample to produce a specimen for electron microscopy and diffraction presents some difficulty, owing to the highly reactive nature of the material. When chemical thinning is used alone, the electron transmitting regions are composed of a variety of complex compounds, presumably complex oxides. A successful polygranular specimen was finally prepared by starting with a 3 mm disc sample which had been electrolytically thinned at approximately 273 K, using a mixture of concentrated H_3PO_4, H_2O_2 and concentrated HF(48%) in the ratio 10:4:1, to the stage of producing a hole in the center. This was then etched in the electron beam of a Siemens Elmiskop 1A, by operating with the low-temperature stage in the presence of a little water vapour. This is a well-known method of specimen etching, which is difficult to utilize in a controlled way, but in this case we were able to produce a fair region of thinned sample with, initially, very little oxide coating. This sample was used to obtain the following results.

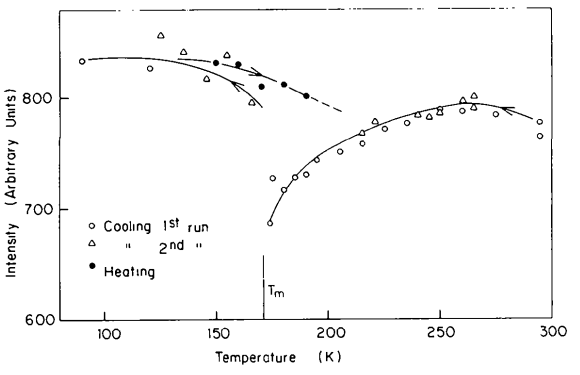

Fig. 1. Neutron diffraction results obtained by Wilkins *et al.* (1982) for the integrated intensity of the 200 reflexion, showing the marked discontinuity occurring at T_m, which exhibits a hysteresis on reversing the direction of temperature change.

III. Electron diffraction data collection

The data were collected on three different instruments, with different types of specimen goniometers. These were the Siemens Elmiskop 1A, the JEOL 200A and the JEOL 200CX electron microscopes. The Siemens Elmiskop was fitted with a specially constructed cold stage capable of operating between room temperature and 173 K both in point diffraction and convergent-beam diffraction modes (Dowell & Williams, 1976). The JEOL 200A operated at room temperature with a normal top-entry goniometer, while the JEOL 200CX was operated with a JEOL single-axis side-entry goniometer designed to operate with specimen temperatures down to 173 K.

IV. Room-temperature data

A series of single-crystal electron diffraction patterns over an angular range was obtained by rotating a crystal away from the [001] zone, approximately about the $[2\bar{2}0]^*$ vector. Most data were obtained at the exact [001] zone axis; in addition, however, observations were made at the [114], [112], [223] and [215] zones.

Fig. 2 shows the [001] point diffraction pattern. This pattern shows streaks through the Bragg reflexions, which run perpendicular to $[2\bar{2}0]^*$ diffraction vectors: *i.e.* all Bragg points display mutually perpendicular streaks in $[220]^*$ and $[2\bar{2}0]^*$ directions. The crystal is not exactly aligned to the zone-axis setting, and it is possible to see that streaking is quite strong some distance from the exact Bragg condition (streaks appear through both weakly and strongly excited reflexions of the same set).

By rotating the crystal to the [114] zone, the radial component of the streaks through the $2\bar{2}0$ diffraction spot almost disappears, leaving a mainly non-radial streak (Fig. 3). This indicates that the *radial* component of streaks visible in Fig. 2 can be attributed to dynamic scattering effects due to the high symmetry of the [001] zone.

It is a significant observation that the streaks observed in Figs. 2 and 3 running through Bragg reflexions are limited to short segments near the

reflexions, and are *not* continuous lines between reflexions, indicating that the diffuse scattering in reciprocal space is not in the form of uniform sheets.

In Fig. 4, with further rotation to the [112] zone, continuous lines between reflexions begin to appear, which are parallel to the $[11\bar{1}]^*$ vector. These are non-radial streaks, *i.e.* they pass through the $2\bar{2}0$–$3\bar{1}\bar{1}$ line of reflexions, but are supressed along the 000–$22\bar{2}$ line. However, the $22\bar{2}$ reflexions have very short non-radial diffuse streak segments in the perpendicular direction. Apparent non-Bragg reflexions appear diffusely for the first time in this series: *i.e.* at the position $\frac{1}{2}(3\bar{1}\bar{1})$, joined by short diffuse segments. Although it would be difficult to interpret this feature from a single pattern, this observation is found to be consistent with the intersection of the Ewald sphere with reciprocal-lattice extensions parallel to the $[\bar{1}11]$ direction (see § VI), by analysing further pictures.

Fig. 5, taken close to the low-symmetry zone of [215], is important to our understanding of the three-dimensional structure of the diffuse scattering, since it indicates rather clearly the segmented nature of the diffuse streaks. At this orientation the $2\bar{2}0$ reflexion is no longer exactly satisfied. A dense diffuse streak replaces the Bragg reflexion, and continues in one direction to the $3\bar{1}\bar{1}$ reflexion but does not appear far outside this $2\bar{2}0$–$3\bar{1}\bar{1}$ reflexion pair. Streak segments appear through several pairs of Bragg reflexions. The main streaks seen in the background run approximately parallel to the $[\bar{1}11]^*$ and $[\bar{1}\bar{1}1]^*$ directions. These out-of-zone vectors project on to the plane of this pattern as $[\bar{5}51]$ and $[\bar{5}\bar{5}3]$, respectively, which

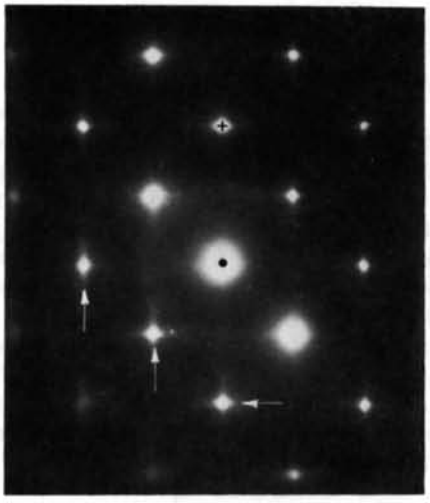

Fig. 2. Room-temperature diffraction pattern close to the [001] zone. Directions of three non-radial streaks are indicated by arrows. In this figure, as in Figs. 3, 4, 7 and 8, the central beam is marked with a ●, and the $2\bar{2}0$ reflexion position is marked with a +. In the series the $[2\bar{2}0]^*$ vector is kept vertical.

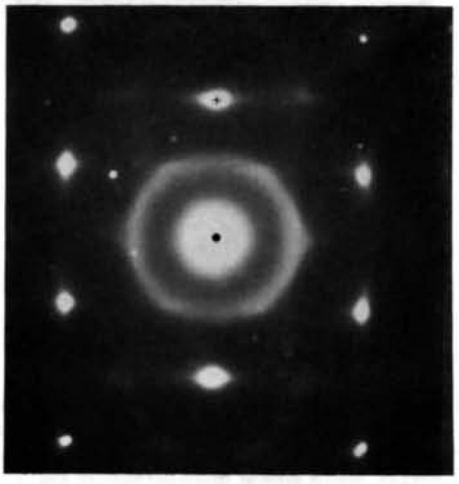

Fig. 3. Room-temperature pattern; [114] zone axis.

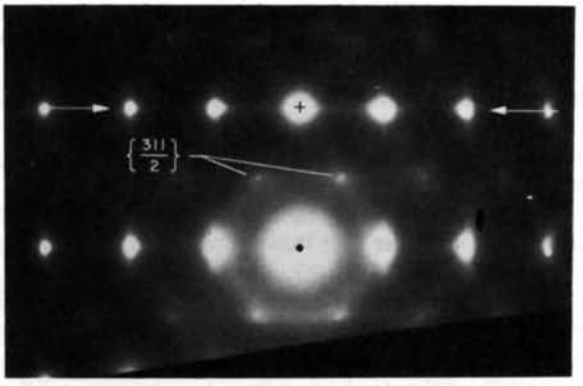

Fig. 4. Room-temperature pattern; [112] zone axis. The $[11\bar{1}]$ line passing through the $2\bar{2}0$-indexed position is indicated by a pair of arrows.

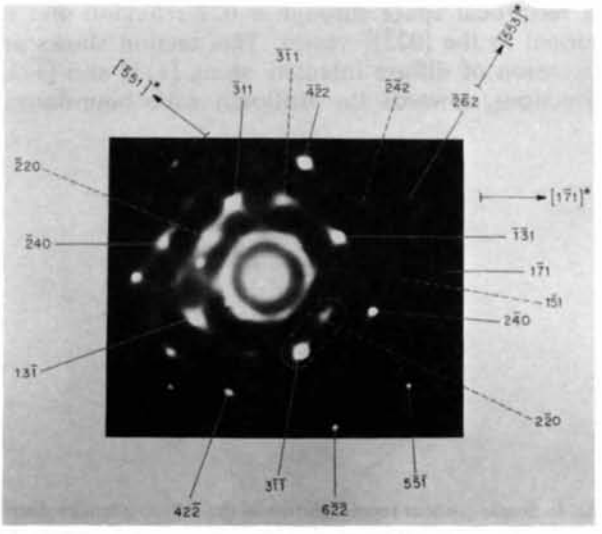

Fig. 5. Room-temperature pattern; [215] zone axis. Reflexion indices are shown around the figure. Full drawn lines indicate reflexions in the [215] zone, broken lines indicate reflexions out of the zone.

are approximately orthogonal. The segmented nature of the streaks could be largely explained by the existence of 111-directed rods in reciprocal space which are intersected at a shallow angle by the Ewald sphere. Observations on individual segments are as follows. Reflexions $\bar{1}31$ and $\bar{3}\bar{1}1$ are joined by a relatively weak line of diffuse scattering, parallel to $[\bar{2}20]^*$. On the other hand, the reflexion pair $3\bar{1}\bar{1}$ and $2\bar{2}0$ are joined by an intense diffuse line segment parallel to $[11\bar{1}]^*$. A detailed indexing, which allows other segments to be analysed, is given with Fig. 5. These observations demonstrate that the line segments between reflexions become increasingly intense as they approach the $[111]^*$ direction. The conclusion to be drawn from this is that, while diffuse *sheets* exist in reciprocal space, perpendicular to the $\langle 220\rangle^*$ vectors, the intensity within the sheets is non-uniform, and rod-like intensification occurs along the $\langle 111\rangle^*$ lines. Finally, the apparent hexagon of segments around the center of the pattern is formed by a weaker third-direction streaking of 111-type. Since $[1\bar{1}1]^*$ passes through the plane of projection at a steeper angle than the vectors $[\bar{1}\bar{1}1]^*$ and $[\bar{1}11]^*$, there is a projected out-of-zone hexagon formed by these segments.

The set of pictures, including that in Fig. 5, are consistent with the fact that more continuous diffuse lines appear as $\langle 111\rangle^*$ directions are approached.

In the later pictures of the above series, notably in Figs. 3, 4 and 5, an oxide coating, which was forming during the course of the investigation, contributes an inner diffuse ring to the patterns; the structural diffuse scattering from the alloy can however still be followed through the series.

Fig. 6 is a schematic summary of the above observations. This diagram shows a section of diffuse intensity in reciprocal space through a $02\bar{2}$ reflexion and is normal to the $[02\bar{2}]^*$ vector. This section shows an extension of diffuse intensity along [111] and $[\bar{1}11]$ directions, towards the Brillouin zone boundaries. The dotted lines in this figure indicate changes which occur as the temperature is lowered (see below).

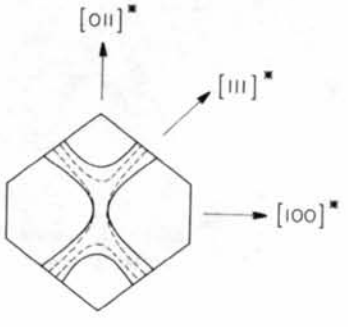

Fig. 6. Single-contour representation of the diffuse intensity distribution in reciprocal space, displayed as a section through the $02\bar{2}$ reflexion, perpendicular to the corresponding $[02\bar{2}]^*$ vector. The full line shows the room-temperature observations; the broken line indicates the contraction towards the fundamental reflexion, observed at low temperature (see text).

V. Low-temperature data

Diffraction data taken below room temperature, at approximately 193 K, on the Siemens stage described above, showed patterns which were not markedly different in appearance from those taken at room temperature. This was attributed to the fact that for the alloy studied (24 at.% Tl) the transition temperature was below the range of the low-temperature stage used. Some distinct differences were noted, however, and these are described below.

Fig. 7 is a focused-point pattern at the [001] zone which is similar to that shown in Fig. 2. The streaks running perpendicular to the $\langle 220\rangle^*$ directions in this pattern, however, are noticeably weaker than those appearing at room temperature in Fig. 2, and are more closely confined to the vicinity of the Bragg reflexions.

Fig. 8 shows a disc pattern, or defocused convergent-beam pattern, for which the convergent-beam probe was focused slightly above the specimen. The orientation corresponds very closely to [112]. When compared with the point pattern Fig. 3, the most noticeable change in going to the new picture is the almost complete *absence* of non-radial streaking parallel to $[11\bar{1}]$. Two possible reasons for this are: firstly, the reduced temperature (near 193 K) of the sample; secondly, the size of the probe. Diffuse scattering arising from static displacements tends to decrease as convergent-beam and fine-probe diffraction conditions are approached, whereas thermal

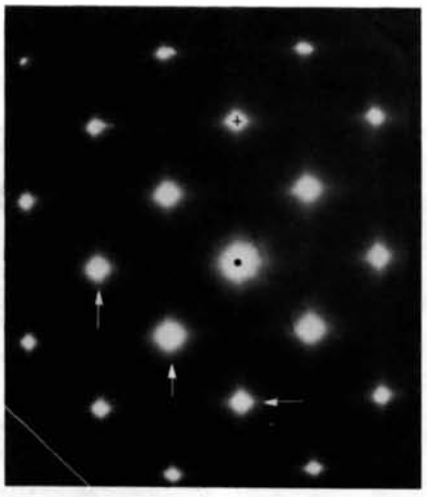

Fig. 7. Low-temperature focused-point diffraction pattern; [001] zone axis, showing slight contraction of diffuse scattering towards the Bragg reflexions. Directions of three non-radial diffuse streaks, which appear more strongly in Fig. 2, are indicated by arrows.

diffuse scattering is not a function of probe size on the specimen (see, for example, Bursill, Dowell, Goodman & Tate, 1978). Equally noticeable in Fig. 8 is the appearance of both sharply-defined and diffusely-defined strong discs at non-Bragg sites, *e.g.* at the $\frac{1}{2}(311)$ position. The sharply-defined reflexions are found to come from a second grain and index as 111 Bragg reflexions, but the diffusely-defined discs appear to come from the same grain giving the [112] zone pattern. These diffuse reflexions can be understood as extensions from the neighboring [111] zone, of $\frac{1}{3}(422)$-type reflexions. These reflexions are those which could arise from a single close packed hexagonal layer, which are space-group forbidden with f.c.c. stacking. Appearance of intensity at these positions is a typical feature of diffraction from stacking-faulted f.c.c. material.

VI. Interpretation

According to Koyama & Nittono (1981) the diffuse scattering in In-(18-30) at.% Tl alloys are {110} sheets through the Bragg reflexions. According to their theory these diffuse sheets are due to thermal vibrations, and in particular to transverse lattice modes. These are said to propagate along ⟨110⟩ atomic chains with a $\langle 1\bar{1}0\rangle$-directed polarization vector. Koyama & Nittono's explanation of the diffuse scattering in the In-Tl alloys is very similar to the interpretation by Honjo, Kodera & Kitamura (1964) for aluminium. In their electron diffraction patterns these authors observed continuous ⟨110⟩ streaks in [001]-orientation patterns. The theory for this kind of thermal diffuse scattering has been further developed by Komatsu & Teramoto (1966) and Kashiwase, Kainuma & Kogiso (1976).

Koyama & Nittono explained the formation of the sheared f.c.t. martensitic phase at T_m in terms of two low-frequency transverse lattice modes. This soft-mode interpretation for the martensitic transformation is in good agreement with the double-shear description given by Bowles, Barrett & Guttman (1950).

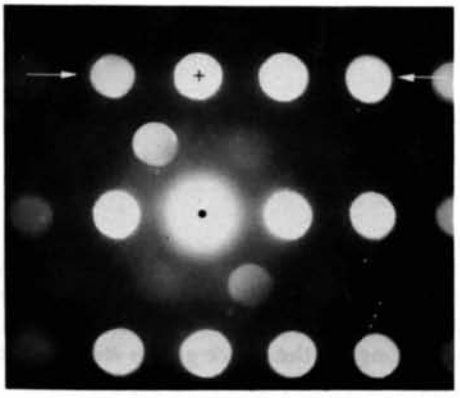

Fig. 8. Low-temperature convergent-beam diffraction pattern; approximate [112] zone-axis setting. The $[11\bar{1}]$ line through the $2\bar{2}0$ reflexion is indicated by arrows, for comparison with that in Fig. 4.

The diffuse scattering found in the present investigation is not in accord with the Koyama & Nittono model in certain significant respects. An exploration of diffuse intensity distribution in reciprocal space has shown that the streaks are continuous along ⟨111⟩ directions, and restricted in extension in other directions (including ⟨110⟩) to the vicinity of the Bragg reflexions. The cubic symmetry (of the high-temperature phase) permitted us to reconstruct a three-dimensional model of the diffuse intensity from relatively few zone-axis patterns. It was also found that elongation of diffuse streaks along ⟨110⟩ directions decreased as the temperature was reduced towards T_m. Fig. 6, which represents a section of reciprocal space through a $02\bar{2}$ reflexion, shows the features of our three-dimensional model, in very schematic form. Here broken lines are used to display the suggested contraction of this streaking at low temperature. In addition to these data, convergent-beam patterns taken with a fine probe allowed us to examine the relative importance, qualitatively, of static displacements as compared with thermal displacements in forming the diffuse streaks found in the selected-area-type point patterns. It seems reasonable that, as compared with the Koyama & Nittono study, static displacements should be more important in our case since we were working with an alloy with a much lower T_m value. There does, however, appear to be a fundamental difference between the interpretations given in these two investigations, although not necessarily any real difference in the electron diffraction data. Fig. 1 of Koyama & Nittono (1981), for example, which is a schematic model of the intensity distributions in the [001] pattern, shows the same segmented nature of diffuse distribution which we have reported for this orientation. In our Figs. 2 and 7 for the [001] axis, it is clear that there is no continuous streaking along any of the directions [100], [110] (nor along the out-of-plane direction [211] which would lead to visible streak extension along the [210] direction of the [001]-zone pattern), and *only* streak *segments* along [110].

VII. Conclusions

The strong tendency for diffuse streaking along ⟨111⟩ directions indicates that the static disorder responsible is within {111} planes. Confirmation of diffuse scattering of such intensity in regions away from the fundamental reflexions would appear to explain the diminution in neutron diffraction intensities observed by Wilkins *et al.* (1982) in the pre-martensitic region (see Fig. 1), since, in their experiment, diffraction

peaks were recorded by collection of scattering over a limited solid angle and a smooth background was subtracted from the 'sharp' peaks. Diffuse scattering in the neighborhood was not investigated.

A previous electron microscopic examination of InTl, which included image observations of a 'mottled' pre-martensitic contrast but recorded a less-extensive survey of reciprocal space than presented here, was made by Lasalmonie & Costa (1979). Their interpretation of results, in terms of static defects, is completely in accord with present conclusions.

On a lattice-dynamic model, coupling between soft modes with polarizations along $[01\bar{1}]$ and $[10\bar{1}]$ directions (having propagation vectors along [011] and [101], respectively) would lead to the observed static displacements in the (111) plane, parallel to $[11\bar{2}]$, upon freezing of these phonons. The absence of diffuse scattering along [100]* directions indicates that phonons with [110] and $[1\bar{1}0]$ lateral displacements are not coupled. From the analysis of Bowles, Barrett & Guttman (1950) it is evident that [111] is an invariant vector during this type of phase transition. This is in complete agreement with observations and the interpretative model presented here. The really surprising result may be that freezing and coupling of phonon modes is so strong more than 170 K above the critical temperature for the martensitic phase transformation.

References

BOWLES, J. S., BARRETT, C. S. & GUTTMAN, L. (1950). *Trans. Am. Inst. Min. Eng.* **188**, 1478-1485.

BURSILL, L. A., DOWELL, W. C. T., GOODMAN, P. & TATE, N. (1978). *Acta Cryst.* A**34**, 296-308.

DOWELL, W. C. T. & WILLIAMS, D. (1976). *Ultramicroscopy*, **1**, 43-48.

GUNTON, D. J. & SAUNDERS, G. A. (1973). *Solid State Commun.* **12**, 569-572.

HONJO, G., KODERA, S. & KITAMURA, N. (1964). *J. Phys. Soc. Jpn*, **19**, 351-367.

KASHIWASE, Y., KAINUMA, Y. & KOGISO, M. (1976). *J. Phys. Soc. Jpn*, **40**, 1707-1719.

KOMATSU, K. & TERAMOTO, K. (1966). *J. Phys. Soc. Jpn*, **21**, 1151-1159.

KOYAMA, Y. & NITTONO, O. (1981). *J. Jpn Inst. Met.* **45**, 869-877.

LASALMONIE, A. & COSTA, P. (1979). *ICOMAT* 79. Proc. 3rd. Int. Conf. on Martensitic Transformations. *Am. Soc. Met.* pp. 100-103.

NAKANISHI, N. (1979). *Prog. Mater. Sci.* **24**, 143-265.

NITTONO, O. & KOYAMA, Y. (1981). *Sci. Rep. Res. Inst. Tohoku Univ. Ser. A*, **29**, Suppl. 1, 53-60.

WILKINS, S. W., LEHMANN, M. S., FINLAYSON, T. R. & SMITH, T. F. (1982). Proc. Int. Conf. on Solid State Phase Transformations, AIME, Pennsylvania, pp. 1235-1239.

Acta Cryst. (1984). B**40**, 560-566

Electron-Microscopic Study of the Structure of Metastable Oxides Formed in the Initial Stage of Copper Oxidation. II. Cu_8O

BY R. GUAN

Department of Applied Physics, Osaka University, 2-1 *Yamadaoka, Suita, Osaka* 565, *Japan and Institute of Metal Research, Academia Sinica, Shenyang, People's Republic of China*

H. HASHIMOTO

Department of Applied Physics, Osaka University, 2-1 *Yamadaoka, Suita, Osaka* 565, *Japan*

AND K. H. KUO

Institute of Metal Research, Academia Sinica, Shanyang, People's Republic of China

(*Received* 5 *March* 1984; *accepted* 3 *July* 1984)

Abstract

Small thin metastable copper oxide crystals with the chemical composition Cu_8O formed on slightly oxidized thin plates and fine particles of copper have been studied by high-resolution electron microscopy. The atomic positions of Cu and O have been determined by the analysis of electron diffraction patterns and comparison of the observed structure images with theoretical ones calculated on the basis of the dynamical theory of electron diffraction and image formation theory. Crystalline Cu_8O is base-centered orthorhombic and belongs to the space group *Bmm*2 with lattice parameters $a = 5{\cdot}47$, $b = 6{\cdot}02$ and $c = 9{\cdot}34$ Å. The unit-cell volume is approximately four times larger than that of Cu_2O. The same oxide has also been found in copper powder which has been stored at room temperature for more than 20 years.

0108-7681/84/060560-07$01.50